

THE PHASES DIFFERENTIAL ASTROMETRY DATA ARCHIVE. V. CANDIDATE SUBSTELLAR COMPANIONS TO BINARY SYSTEMS

MATTHEW W. MUTERSPAUGH^{1,2}, BENJAMIN F. LANE³, S. R. KULKARNI⁴, MACIEJ KONACKI^{5,6}, BERNARD F. BURKE⁷,
M. M. COLAVITA⁸, M. SHAO⁸, WILLIAM I. HARTKOPF⁹, ALAN P. BOSS¹⁰, AND M. WILLIAMSON²

¹ Department of Mathematics and Physics, College of Arts and Sciences, Tennessee State University,
Boswell Science Hall, Nashville, TN 37209, USA; matthew1@coe.tsuniv.edu

² Tennessee State University, Center of Excellence in Information Systems, 3500 John A. Merritt Blvd., Box No. 9501, Nashville, TN 37209-1561, USA

³ Draper Laboratory, 555 Technology Square, Cambridge, MA 02139-3563, USA; blane@draper.com

⁴ Division of Physics, Mathematics and Astronomy, 105-24, California Institute of Technology, Pasadena, CA 91125, USA

⁵ Nicolaus Copernicus Astronomical Center, Polish Academy of Sciences, Rabianska 8, 87-100 Torun, Poland; maciej@ncac.torun.pl

⁶ Astronomical Observatory, Adam Mickiewicz University, ul. Sloneczna 36, 60-286 Poznan, Poland

⁷ MIT Kavli Institute for Astrophysics and Space Research, MIT Department of Physics, 70 Vassar Street, Cambridge, MA 02139, USA

⁸ Jet Propulsion Laboratory, California Institute of Technology, 4800 Oak Grove Dr., Pasadena, CA 91109, USA

⁹ U.S. Naval Observatory, 3450 Massachusetts Avenue, NW, Washington, DC 20392-5420, USA

¹⁰ Department of Terrestrial Magnetism, Carnegie Institution of Washington, 5241 Broad Branch Road, NW, Washington, DC 20015-1305, USA

Received 2010 July 8; accepted 2010 September 4; published 2010 October 20

ABSTRACT

The Palomar High-precision Astrometric Search for Exoplanet Systems monitored 51 subarcsecond binary systems to evaluate whether tertiary companions as small as Jovian planets orbited either the primary or secondary stars, perturbing their otherwise smooth Keplerian motions. Six binaries are presented that show evidence of substellar companions orbiting either the primary or secondary star. Of these six systems, the likelihoods of two of the detected perturbations to represent real objects are considered to be “high confidence,” while the remaining four systems are less certain and will require continued observations for confirmation.

Key words: astrometry – binaries: close – binaries: visual – techniques: interferometric

Online-only material: machine-readable and VO tables

1. INTRODUCTION

The use of astrometric measurements to detect the reflex motions of stars caused by substellar companions orbiting them has a long history filled with false alarms. Famously, van de Kamp (1963) claimed to have discovered giant planet companions to Barnard’s Star. His first estimates of a single planet of 1.6 times the mass of Jupiter with an orbital period of 24 years and an eccentricity of 0.6 later revised to two planets with orbital masses and periods of $1.1 M_J$ at 26 years and $0.8 M_J$ at 12 years (van de Kamp 1969). He never accepted growing evidence from other astronomers that these discoveries were not repeatable elsewhere (Gatewood & Eichhorn 1973; Hershey 1973); today it has been shown conclusively that these planets are not real (Kürster et al. 2003).

Han et al. (2001) used *Hipparcos* measurements to analyze stars with known radial velocity (RV) detected exoplanet candidates. The precision of *Hipparcos* was insufficient to detect the reflex motions if the objects are in fact planets; however, if instead the orbits are face-on, the actual companion masses would be larger than the RV-derived masses, so the resulting much larger motions could have been detected by *Hipparcos*. This provided a test of whether the RV candidates were in fact mostly face-on binaries (transiting planets prove that at least some RV candidates are real planets—see, for example, Henry et al. 2000—but this is not applicable to the vast majority of systems). Han et al. (2001) concluded that most RV candidates *did* show orbital motions in the *Hipparcos* database, and were thus binary stars, not planetary systems. However, Pourbaix (2001) showed the orbital analysis to be incorrect, and a proper statistical analysis reveals no credible detections; instead the results

are consistent with randomly oriented orbits and most of the RV-detected objects being planetary in nature.

A few RV-detected planetary systems have had their orbital geometries constrained by *Hubble Space Telescope* astrometry (Benedict et al. 2002; McArthur et al. 2010). Though impressive work, these do not represent discoveries of new systems by astrometry, and the ratio of measurement precision to signal amplitude is low enough to make it unlikely the astrometry could have produced a detection by itself (or even have been made, given the time requirements of a blind search with *Hubble*) had the RV detection not already been present. Pravdo et al. (2005) successfully used astrometry to discover a brown dwarf companion to an M dwarf, a promising first step on the path to finding true planets. The brown dwarf was later confirmed by direct imaging (Lloyd et al. 2006). Most recently, Pravdo & Shaklan (2009) claimed an astrometric detection of a giant planet around a nearby M dwarf from the STEPS project, using standard CCD astrometry from large aperture telescopes. However, this candidate was rapidly shown to be inconsistent with RV observations by Bean et al. (2010).

It is thus with some trepidation that we announce the candidate substellar companions orbiting either the primary or secondary stars in several binaries studied using differential astrometry by PHASES—the Palomar High-precision Astrometric Search for Exoplanet Systems. Given that other astrometrically “discovered” substellar objects have not withstood the test of continued observations, these may represent either the first such companions detected, or the latest in the tragic history of this challenging approach.

Given the challenges of astrometry, why would it be considered a preferred way to detect planets in current and future

searches? Astrometry has a number of advantages over other techniques.

1. Astrometry and RV provide information about the masses of companions to nearby stars. Other methods are insensitive to this fundamental property.
 - (a) Because the reflex motion of the star is monitored, the mass of the companion is measured directly. For nearby systems that can be followed up by direct imaging, only RV and astrometry provide such information.
 - (b) The two-dimensional nature of the astrometric measurement provides unique mass estimates. In contrast, RV detections only give the companion mass times the sine of the unknown inclination, $M \sin i$.
2. Astrometry is effective in regimes where RV has reduced precision:
 - (a) Astrometry can operate over a wide range of stellar masses, rotational velocities, and spectral types to better explore relationships between the properties of the host star and its planetary system. RV is most effective for slowly rotating, mid-to-late-type stars.
 - (b) Astrometric sensitivity increases with companion period, an opposite trend as RV. This is particularly important when identifying long-period planets for direct imaging work, where the wider star–planet separation reduces technical challenges for imaging.
 - (c) Astrometry is less sensitive to surface vibrations and star spots than RV (Makarov et al. 2009). This is particularly important for identifying the small ($1 \mu\text{as}$ and 0.1 m s^{-1}) signals of Earthlike planets in the habitable zones of nearby, Sunlike stars. This motivates future astrometric planet searches.
 - (d) Astrometry is well suited to studying planets in binary systems. This is the primary motivation for using the astrometric method for PHASES. RV can study planetary companions to a few binary systems. For example, binaries with very large sky separations can be studied, which frequently implies large physical separations as well, and these evolve rather like single stars, revealing little new about planetary system formation and evolution.

It is instead binaries with separations in the critical $\sim 10\text{--}50$ AU range that can greatly contribute new information. This range is wide enough that planets can have stable orbits around either star if present, but close enough that the second star may influence formation of the planet in the first place. RV can study a few special cases of these binaries: those very close to the solar system (e.g., γ Cep; Campbell et al. 1988; Hatzes et al. 2003) so the components are spatially resolved, a few high contrast systems (such that the second star minimally impacts the spectrum; e.g., HD 126614; Howard et al. 2010), and a few triple star systems, where a short-period stellar subsystem causes the spectral features to be split (e.g., the controversial companion to HD 188753; Konacki 2005a). In other cases, the stars are often both spatially unresolved and spectrally blended, making precision velocities impossible; even when the lines can be separated, precision RV on the double spectrum is challenging (Konacki 2005b).

Thus, PHASES used astrometry to observe 51 binary systems with the goal of identifying new tertiary companions orbiting

either of the bright stars in the system. Of these, 33 systems have more than 10 successful observations, allowing a realistic chance for a companion search to be successful. Seven of those 33 systems are either triple or quadruple stars, five more are so distant that their physical separations fall well outside of the 50 AU limit (two of these—HD 171779 and HD 221673—may have brown dwarf companions, and are presented in this paper), and six more have semimajor axes less than 10 AU, though these last two classes are useful to verify the astrometric technique. The remaining 15 systems provide a sample from which the frequency of planets in closely separated binaries can be evaluated. Pfahl & Muterspaugh (2006) showed that stellar encounters, even in star-forming regions where the stellar density is higher than typical space, are rare enough that only $\sim 0.1\%$ of closely separated binaries could pick up a planet that had not originally formed as a companion in the binary itself but rather via an exchange or binary hardening event. Observed frequencies of planets in close binaries that are higher than this value offer evidence of in situ formation. If giant planets do form in these binaries, it is likely the process must be rapid. Current core-accretion models predict slow formation, though the competing gravitational instability method shows promise at rapid formation. Thus, the frequency of planet formation in these close binaries evaluates the relative frequencies with which these (and other) modes of giant planet formation occur in nature.

Unfortunately, the statistics of the number of binaries that have been observed by RV are difficult to evaluate. However, several planets have been found in close binaries by RV methods, certainly more than the 0.1% frequency predicted by non-in situ formation; see Table 1. The next challenge is to evaluate the planet frequency in a less biased manner. Though limited in size, the PHASES sample represents an attempt to contribute to this effort.

This paper is the fifth in a series, analyzing the final results of the PHASES project after its completion in late 2008. The first paper describes the observing method, sources of measurement uncertainties, limits of observing precisions, derives empirical scaling rules to account for noise sources beyond those predicted by the standard reduction algorithms, and presents the full catalog of astrometric measurements from PHASES (Muterspaugh et al. 2010d). The second paper combines PHASES astrometry with astrometric measurements made by other methods as well as RV observations (when available) to determine orbital solutions to the binaries' Keplerian motions, determining physical properties such as component masses and system distance when possible (Muterspaugh et al. 2010b). The third paper presents limits on the existence of substellar tertiary companions, orbiting either the primary or secondary stars in those systems, that are found to be consistent with being simple binaries (Muterspaugh et al. 2010c). The fourth paper presents three-component orbital solutions to a known triple star system (63 Gem A = HD 58728) and a newly discovered triple system (HR 2896 = HD 60318) Muterspaugh et al. (2010a). Finally, the current paper presents candidate substellar companions to PHASES binaries as detected by astrometry.

Astrometric measurements were made as part of the PHASES program at the Palomar Testbed Interferometer (PTI; Colavita et al. 1999), which was located on Palomar Mountain near San Diego, California. It was developed by the Jet Propulsion Laboratory, California Institute of Technology for NASA, as a testbed for interferometric techniques applicable to the Keck Interferometer and other missions such as the *Space Interferom-*

Table 1
Close Binaries with Substellar Companions

System	Object Type ^a	a (AU)	e^b	M_1/M_2^c	R_t (AU) ^d	References
γ Cephei	p	18.5	0.36	1.59/0.34	3.6	1, 2
GJ 86 ^e	p	~ 20	...	0.7/1.0	~ 5	3, 4, 5
HD 41004	p	~ 20	...	0.7/0.4	~ 6	6
HD 41004	bd	~ 20	...	0.4/0.7	~ 5	6
HD 126614	p	~ 45	...	1.145/0.324	~ 15	7
HD 188753 ^f	p	12.3	0.50	1.06/1.63	1.3	8, 9, 10
HD 196885	p	~ 25	...	1.3/0.6	~ 8	11
HD 176051	p	19.1	0.2667	0.71/1.07	3.2	This work
HD 221673	bd	95	0.322	2/2	12.6	This work

Notes.

^a “p” indicates a giant planet companion and “bd” indicates the companion is a brown dwarf.

^b When the eccentricity is unknown, the projected binary separation is used as an approximation, except in the case of HD 126614, where a linear velocity trend is observed, and the binary itself has been resolved, leading to two possible solutions with $a = 40_{-4}^{+7}$ and 50_{-3}^{+2} AU.

^c Mass of star hosting planet divided by mass of the companion star (in solar masses).

^d The distance from the primary star at which a disk would be rapidly truncated by tides (Pichardo et al. 2005).

^e The companion star is a white dwarf of mass $\simeq 0.5 M_{\odot}$. To estimate R_t at the time of formation, an original companion mass of $1 M_{\odot}$ is assumed.

^f The companion star itself is a binary with semimajor axis 0.67 AU. This candidate is controversial due to minimal data in the discovery paper with sporadic observing cadence and a lack of evidence found by Eggenberger et al. (2007) and Mazeh et al. (2009).

References. (1) Campbell et al. 1988; (2) Hatzes et al. 2003; (3) Queloz et al. 2000; (4) Mugrauer & Neuhauser 2005; (5) Lagrange et al. 2006; (6) Zucker et al. 2004; (7) Howard et al. 2010; (8) Konacki 2005a; (9) Eggenberger et al. 2007; (10) Mazeh et al. 2009; (11) Correia et al. 2005.

etry Mission (SIM). It operated in the J ($1.2 \mu\text{m}$), H ($1.6 \mu\text{m}$), and K ($2.2 \mu\text{m}$) bands, and combined starlight from two out of three available 40 cm apertures. The apertures formed a triangle with one 110 m and two 87 m baselines. PHASES observations began in 2002 continued through 2008 November when PTI ceased routine operations.

2. ALGORITHM FOR IDENTIFYING ASTROMETRIC COMPANIONS

Blind searches were conducted to identify potential tertiary companions to the PHASES binaries. An algorithm based on that of Cumming et al. (1999, 2008) was modified for use on astrometric data for binary systems, as described in Paper III, and used to conduct blind searches for tertiary companions in these systems.

The overall procedure is to create a periodogram of an F statistic comparing the goodness-of-fit χ^2 between a single Keplerian model and that for a double Keplerian model for a number of possible orbital periods for the second orbit. The orbital periods selected were chosen to be more than Nyquist sampled, to ensure complete coverage, as $P = 2fT/k$ where T is the span of PHASES observations, $f = 3$ is an oversampling factor, and k is a positive integer. Two searches were conducted for each binary: first, with the use of only the PHASES measurements, and second with both the PHASES and non-PHASES astrometry, to better constrain the wide binary motion during the search. In addition to the positive integer values of k , the period corresponding to $k = 1/2$ was evaluated to search for companions with orbits slightly longer than the PHASES span.

The orbital period for which the F statistic periodogram has its maximum value is the most likely orbital period of a companion object. To ensure the peak is a real object rather than a statistical fluctuation, 1000 synthetic data sets with identical cadence and

Table 2
Number of PHASES and Non-PHASES Measurements and Unit Weight Uncertainties for Non-PHASES Measurements

HD Number	N_P	$N_{P,O}$	N_{NP}	$N_{NP,O}$	$\sigma_{\rho,\circ}$	$\sigma_{\theta,\circ}$
13872	89	0	103	14	0.013	2.51
171779	54	0	128	12	0.020	2.79
176051	65	1	327	12	0.140	4.48
196524	72	1	598	48	0.046	2.78
202444	39	0	286	13	0.123	4.37
221673	98	1	333	21	0.056	2.12

Notes. The numbers of PHASES and non-PHASES astrometric measurements used for orbit fitting with each of the binaries being studied are presented in Columns 2 and 4, respectively, along with the additional numbers of measurements rejected as outliers in Columns 3 and 5. Columns 6 and 7 list the 1σ measurement uncertainties for unit weight measurements from non-PHASES observations determined by iterating Keplerian fits to the measurements with removal of 3σ or greater outliers in either dimension. Columns 6 and 7 are in units of arcseconds and degrees, respectively.

measurement uncertainties as the actual data were created and evaluated in the same manner. The fraction of these having a maximum F statistic larger than that of the actual data provided an estimate of the false alarm probability (FAP) that the signal is not caused by an actual companion.

3. PHASES MEASUREMENTS

PHASES differential astrometric measurements were obtained with the observing method and standard data analysis pipeline described in Paper I. The measurements themselves and associated measurement uncertainties are also tabulated in Paper I. The number of PHASES measurements available for each of the six systems being investigated are listed in Table 2.

Table 3
Non-PHASES Astrometric Measurements

HD Number	Date (year)	ρ (arcsec)	θ (deg)	σ_ρ (arcsec)	σ_θ (deg)	Weight	Outlier
13872	1965.9100	0.250	49.70	0.015	2.81	0.8	1
13872	1966.1100	0.230	50.70	0.029	5.61	0.2	0
13872	1966.7200	0.220	42.80	0.012	2.29	1.2	0
13872	1967.0699	0.190	39.50	0.016	3.00	0.7	0
221673	2006.7170	0.560	98.20	0.102	3.87	0.3	0
221673	2006.9750	0.554	97.70	0.030	1.13	3.5	0
221673	2007.2800	0.580	99.20	0.040	1.50	2.0	0
221673	2008.8850	0.540	100.45	0.018	0.69	9.5	0

Notes. Non-PHASES astrometric measurements from the WDS Catalog are listed with 1σ measurements, uncertainties, and weights. Column 1 is the HD catalog number of the target star, Column 2 is the decimal year of the observation, Columns 3 and 4 are the separation in arcseconds and position angle in degrees, respectively, Columns 5 and 6 are the 1σ uncertainties in the measured quantities from Columns 3 and 4, Column 7 is the weight assigned to the measurement, and Column 8 is 1 if the measurement is a $>3\sigma$ outlier and omitted from the fit, 0 otherwise. The complete table can be found in electronic form in the online version of this journal.

(This table is available in its entirety in machine-readable and Virtual Observatory (VO) forms in the online journal. A portion is shown here for guidance regarding its form and content.)

4. NON-PHASES ASTROMETRY

Measurements of binaries observed by PHASES made by previous astrometric techniques and cataloged in the Washington Double Star Catalog (WDS; Mason et al. 2001, 2010) were assigned weights according to the formula described by Hartkopf et al. (2001). These allowed refined planet searches in which the binary orbit itself is better constrained by the longer duration, though lower precision, astrometric measurements. Including these measurements lifts some degeneracies in the double-orbit modeling.

Unit weight uncertainties in separation and position angle were evaluated by the following iterative procedure. First, guess values for the unit uncertainties of 24 mas in separation and $1^\circ.8$ in position angle were assigned to the measurements of a given binary; these values corresponded to previous experience using this procedure on μ Ori (Muterspaugh et al. 2008). Second, the measurements were fit to a Keplerian model and the orbital parameters were optimized to minimize the fit χ^2 . This intrinsically assumes the non-PHASES astrometric measurements are insensitive to the tertiary companions being sought, an assumption that will be justified given the small sizes of the perturbations detected. Third, the weighted scatter of the residuals in separation and position angle were evaluated, and the guessed unit uncertainties updated to make the rms scatter in each equal to unity. Fourth, the second and third steps were iterated two more times, at which point the values converged. Fifth, the final unit uncertainties were multiplied by the square root of the reduced χ^2 ($\sqrt{\chi_r^2}$) of the fit, and refit one more time with these slightly larger weights. Sixth, if no residuals deviated by more than 3σ , the process ended, otherwise, the single measurement with the largest separation or position angle residual (weighted by its uncertainty) was flagged as an outlier, and removed from future fits. Seventh, the process was repeated at the first step. The resulting weights are listed in Table 2 and the measurements themselves are listed in Table 3.

5. SUBSTELLAR COMPANIONS WITH HIGH DEGREES OF CONFIDENCE

5.1. HD 176051

HD 176051 (HR 7162, HIP 93017, WDS 18570 + 3254, and, though rarely used, the proper name of Inrakluk has been proposed) is an intriguing PHASES binary because its components are relatively low mass (1.07 and $0.71 M_\odot$), and the system is relatively nearby (14.99 ± 0.13 pc) as determined by *Hipparcos* observations (Söderhjelm 1999, hereafter S99). Both of these qualities indicate astrometric perturbations by tertiary companions will have relatively large signals. The model of Holman & Wiegert (1999) (hereafter HW99) for determining which planetary orbits in binary systems are stable long-term predicts companions with periods as long as ~ 3000 days can have stable orbits.

The initial PHASES-only search for companions found a most significant peak of $z = 15.0$ at a period of 581 days with FAP 0.0%. This low value inspired a revised search including both the PHASES and lower-precision non-PHASES astrometric observations to investigate whether the detection continued to be valid. The revised search finds the most significant peak of $z = 63.1$ at a period of 1004 days with FAP 0.0%. These two distinct orbital periods are probably aliases of each other and both are present in both periodograms; see Figure 1.

The two peaks may indicate aliasing, orbital eccentricity, or confusion with the wide binary orbit. Both companion orbital periods were further explored using a double Keplerian model optimizing all orbital elements, including the companion orbital period and allowing for non-circular companion orbits. Both the fit χ^2 and visual inspection of the orbital solution confirmed that the longer period solution is more likely to be correct and the other is a harmonic. Additionally, smaller peaks corresponding to 276, 225, and 7 days were also explored, but did not produce convincing solutions at all.

The eccentricity of the subsystem orbit is not constrained by the astrometry measurements. This is likely due to the PHASES measurements being high precision only in one dimension, making it difficult to use Kepler's second law to lift ambiguity between inclined circular orbits and face-on eccentric ones. The eccentricity is fixed at zero in the present analysis.

The best-fit Keplerian stellar binary+circular subsystem orbital solution is presented in Table 4 and Figure 2. The substellar object is a planet 1.5 ± 0.3 times the mass of Jupiter, assuming a distance of 15 pc and a stellar mass of $0.71 M_\odot$, both based on the *Hipparcos* analysis by S99. If the planet is instead around the more massive star, the planet's mass would be twice as large.

Interestingly, the binary and planetary orbits may be nearly coplanar. The mutual inclination Φ of two orbits is given by

$$\cos \Phi = \cos i_1 \cos i_2 + \sin i_1 \sin i_2 \cos (\Omega_1 - \Omega_2), \quad (1)$$

where i_1 and i_2 are the orbital inclinations and Ω_1 and Ω_2 are the longitudes of the ascending nodes. When RV measurements are not available, there exists ambiguity in which node is ascending, and two different values of the mutual inclination are possible (corresponding to $\Omega_1 - \Omega_2$ varying by 180°). In this case, the two possibilities are $\Phi = 18 \pm 17$ degrees or $\Phi = 126.4 \pm 6.6$ degrees.

5.2. HD 221673

HD 221673 (72 Peg, HR 8943, HIP 116310, WDS 23340 + 3120) is a pair of mid-K giants. Baize (1962) flagged it as

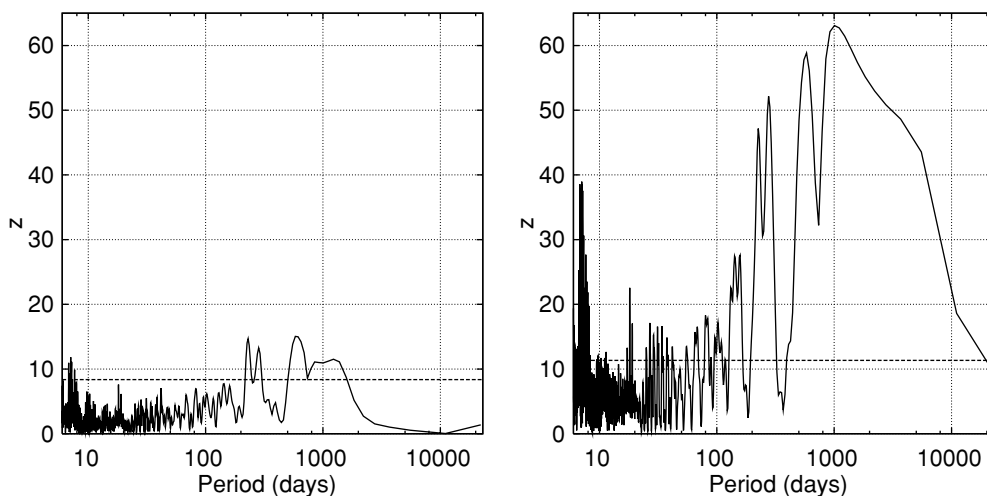


Figure 1. Periodograms of the F statistic comparing models with and without tertiary companions to HD 176051 (HR 7162) in astrometric-only models. The left figure is for analysis only using the PHASES data, while the right is for combined analysis of PHASES and non-PHASES astrometric measurements. For HD 176051 the 1% FAP is at $z = 8.37$ for the PHASES-only analysis, and $z = 11.33$ for the combined analysis, as indicated by horizontal lines.

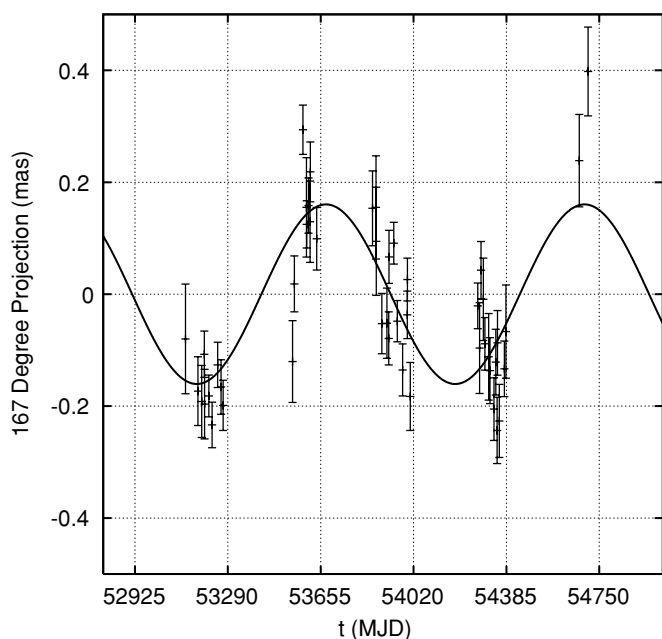


Figure 2. Time series of PHASES observations of HD 176051 (HR 7162) for the 1016 day subsystem orbital solution, measured along an axis at angle 167° from increasing differential right ascension through increasing differential declination; it was along this axis that the PHASES measurements are typically most sensitive. For clarity, only measurements with uncertainties along this axis of $100 \mu\text{as}$ along this axis are shown.

possibly containing a variable star based on the scatter in the differential magnitude measurements by various observers. However, *Hipparcos* photometry shows a scatter of only 6 mmag. The revised *Hipparcos*-based parallax is $5.94 \pm 0.45 \text{ mas}$ (van Leeuwen 2007). This parallax and the best-fit single Keplerian model predict an average stellar mass of $2 M_\odot$. Its long orbital period (~ 800 years) implies a large range of orbits in which companions can be stable—up to 47 years according to the criteria of HW99. Thus, binary dynamics are expected to have a smaller impact on planet formation in this system than others.

HD 221673 is extremely bright at infrared wavelengths ($K = 1.76$), is observable for long stretches during the late summer/fall months of best weather at Palomar, and served as

Table 4
Orbit Model for HD 176051

Parameter	Value	Uncertainty
P_{A-B} (days)	22430	15
T_{A-B} (MHJD)	41384	23
e_{A-B}	0.2667	0.0022
a_{A-B} (arcsec)	1.2756	0.0023
i_{A-B} (deg)	114.159	0.078
ω_{A-B} (deg)	281.71	0.26
Ω_{A-B} (deg)	48.846	0.093
P_{Ba-Bb} (days)	1016	40
T_{Ba-Bb} (MHJD)	53583	39
e_{Ba-Bb}	0	(Fixed)
a_{COL} (μas)	241	41
i_{Ba-Bb} (deg)	115.8	8.2
ω_{Ba-Bb} (deg)	0	(Fixed)
$\Omega_{Ba-Bb,1}$ (deg)	69	11
χ^2 and dof	1015.3	772

Note. Best-fit orbital elements in the Campbell basis for HD 176051, with 1σ uncertainties.

one of the easiest and most reliable PHASES targets to observe. As a result, 98 PHASES measurements were successfully taken of HD 221673. Despite there being large amounts of data available, single Keplerian orbit fitting was frustrated from the early beginnings—the data show much more scatter than predicted by the measurement uncertainties.

The initial PHASES-only search for companions found a most significant peak of $z = 32.9$ at a period of 1276 days ($k = 9$) with FAP 0.0%. This low value inspired a revised search including both the PHASES and lower-precision non-PHASES astrometric observations to investigate whether the detection continued to be valid. The revised search finds a most significant peak of $z = 95.9$ at a period of 1435 days ($k = 8$, within one sample of the peak value for the PHASES-only search) with FAP 0.0%. The periodograms are plotted in Figure 3.

A few single-component RV measurements of 72 Peg have been published by Tokovinin & Smekhov (2002) and Abt et al. (1980). However, the relatively small number and short time coverage of each RV data set reduces any impact they have on constraining either the binary orbit or confirming the existence of additional components (especially low-mass, long-period

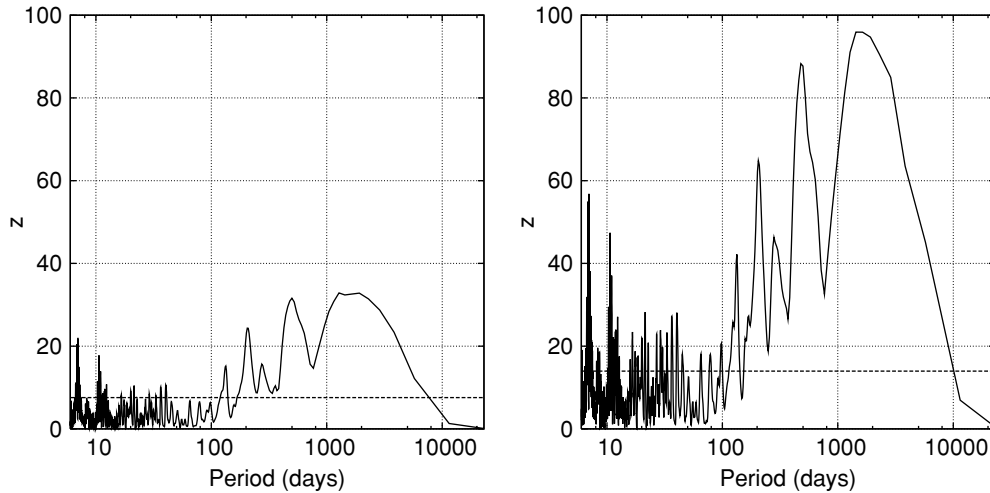


Figure 3. Periodograms of the F statistic comparing models with and without tertiary companions to HD 221673 (72 Peg) in astrometric-only models. The left figure is for analysis only using the PHASES data, while the right is for combined analysis of PHASES and non-PHASES astrometric measurements. For HD 221673 the 1% FAP is at $z = 7.56$ for the PHASES-only analysis, and $z = 13.96$ for the combined analysis, as indicated by horizontal lines.

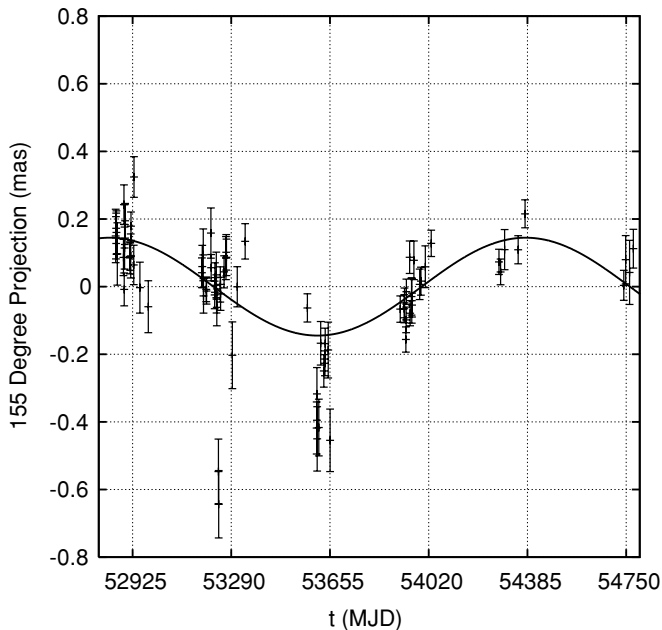


Figure 4. Time series of PHASES observations of HD 221673 (72 Peg) for the 1539 day subsystem orbital solution, measured along an axis at angle 155° from increasing differential right ascension through increasing differential declination; it was along this axis that the PHASES measurements were typically most sensitive for this system. For clarity, only measurements with uncertainties along this axis of $100 \mu\text{as}$ or less are shown.

companions). Neither set shows variation in the velocities and as a result is not used in the orbital analysis.

A refined fit to the astrometric measurements was made for each of the three most significant peaks in the periodogram—the companion orbital period was seeded with values of 1435, 478, and 205 days. Both circular and full Keplerian models were attempted as the companion orbit for each of the three periods being explored. The longest period corresponded to the best fit of the three, though the companion’s eccentricity was not constrained. The best-fit circular model converged with an orbital period of 1539 days and $\chi^2 = 1549.2$, with 850 degrees of freedom, and is presented in Table 5 and Figure 4. While χ^2 is larger than the number of degrees of freedom, it is significantly

Table 5
Orbit Model for HD 221673

Parameter	Value	Uncertainty
P_{A-B} (days)	179811	27745
T_{A-B} (MHJD)	16818	3658
e_{A-B}	0.322	0.047
a_{A-B} (arcsec)	0.568	0.065
i_{A-B} (deg)	21.7	8.3
ω_{A-B} (deg)	293	15
Ω_{A-B} (deg)	56.2	6.0
P_{Ba-Bb} (days)	1539	51
T_{Ba-Bb} (MHJD)	53356	32
e_{Ba-Bb}	0	(Fixed)
a_{COL} (μas)	322	29
i_{Ba-Bb} (deg)	66.6	4.0
ω_{Ba-Bb} (deg)	0	(Fixed)
$\Omega_{Ba-Bb,1}$ (deg)	128.3	4.1
χ^2 and dof	1549.2	850

Note. Best-fit orbital elements in the Campbell basis for HD 221673, with 1σ uncertainties.

improved compared to the model without a tertiary companion, for which $\chi^2 = 2669.9$ with 855 degrees of freedom. The 1539 day companion is a brown dwarf with 35 ± 4 times the mass of Jupiter.

However, the remaining scatter and presence of other peaks in the periodogram (especially that at 478 days) leads one to question whether adding yet another Keplerian representing a fourth component to the system would yet further improve the fit. A 3-Keplerian fit was seeded with the best parameters from the three-component, 2-Keplerian model, as well as the best orbit for a 478 day companion as determined by the initial search. First, both subsystem orbits were assumed to be circular. This led to an improvement in the fit from $\chi^2 = 1549.2$ with 850 degrees of freedom for the 2-Keplerian model to $\chi^2 = 1422.9$ with 845 degrees of freedom for that with three Keplerians summed by superposition. This is only a modest improvement, and at this time no detection is claimed for a second unseen object. Alternatively, the remaining scatter could be related to the 6 mmag photometric variability.

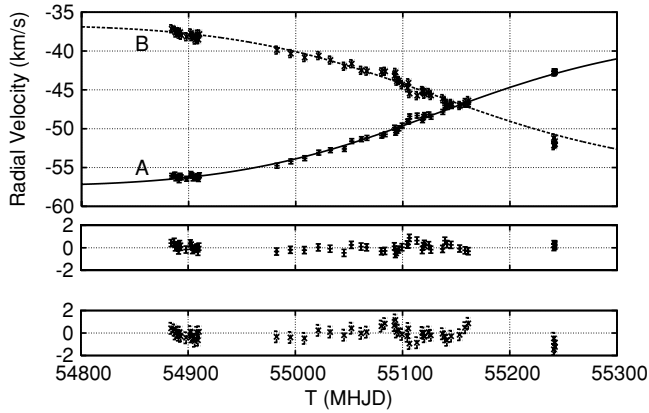


Figure 5. RV orbit of the 21 Ari binary with measurements from TSU’s AST. These measurements enable the binary mass ratio and component masses to be measured, but lack the precision necessary to confirm the presence of a planetary companion. The velocities of both components are shown in the top graph, where the individual components A and B are labeled. The middle graph shows the measurement residuals for component A, and the bottom graph those for component B.

6. SUBSTELLAR COMPANIONS WITH REDUCED LEVELS OF CONFIDENCE

6.1. HD 13872

HD 13872 (21 Ari, HR 657, HIP 10535, WDS 02157 + 2503) is a bright star with mid-F dwarf spectrum. In 1967, it was realized to be a visual binary system with separation less than an arcsecond and roughly equal luminosities by Cousteau. Since its first orbit determination, there have been questions as to whether its spectral type fit the total system mass as measured by the orbit. Cousteau & Morel (1982) proposed that an additional component must exist in the system to explain the overly large total mass. However, their estimate for the total mass was in error due to too small a value of the parallax (of 15 mas). Tokovinin (1987) pointed out that a parallax of 20.1 mas would give a normal sum of masses, a parallax later confirmed by *Hipparcos* (Perryman et al. 1997). However, this is only the case if the star’s mass ratio is near unity, which had not been determined previous to the current investigation, in which a mass ratio $M_B/M_A = 1.027 \pm 0.032$ has been measured.

Fifty-one RV measurements of HD 13872 were made with Tennessee State University’s 2 m Automated Spectroscopic Telescope (AST; Eaton & Williamson 2007) and echelle spectrograph to obtain the stellar mass ratio and better constrain the binary orbit. These measurements are listed in Table 6. The standard data reduction pipeline for determining binary star velocities from AST data was used, as described in Paper II. The RV orbit is plotted in Figure 5.

The initial PHASES-only search for companions found a most significant peak of $z = 6.73$ at a period of ~ 770 days with FAP 3.0%. This relatively low value inspired a revised search including both the PHASES and lower precision non-PHASES astrometric observations, to investigate whether the detection continued to be valid. The revised search finds a most significant peak of $z = 7.49$ at a period of ~ 1284 days with FAP 0.3%. The non-zero FAP, especially when only the PHASES measurements are considered, prevents identification of this as being counted among the strongest of candidates, but is an intriguing possibility, since it would correspond to a giant planet. The periodograms are plotted in Figure 6.

Orbit fitting was refined by allowing the companion orbital period to be optimized, non-circular orbits to be considered,

Table 6
AST Velocities of 21 Ari

Day (HMJD)	RV_A (km s^{-1})	$\sigma_{RV,A}$ (km s^{-1})	RV_B (km s^{-1})	$\sigma_{RV,B}$ (km s^{-1})
54884.158	-56.07	0.31	-37.13	0.50
54887.098	-55.91	0.31	-37.31	0.50
54888.089	-56.39	0.31	-37.68	0.50
54890.089	-56.22	0.31	-37.55	0.50
54891.094	-56.63	0.31	-37.83	0.50
54892.111	-56.05	0.31	-37.57	0.50
54893.096	-56.27	0.31	-37.96	0.50
54898.123	-56.45	0.31	-38.16	0.50
54902.111	-55.84	0.31	-37.67	0.50
54903.111	-56.02	0.31	-38.15	0.50
54904.125	-56.40	0.31	-38.06	0.50
54906.110	-56.26	0.31	-38.58	0.50
54908.110	-56.11	0.31	-37.83	0.50
54909.117	-56.48	0.31	-38.54	0.50
54910.110	-56.00	0.31	-37.81	0.50
54982.467	-54.77	0.31	-39.88	0.50
54995.464	-54.21	0.31	-40.33	0.50
55008.401	-53.80	0.31	-40.84	0.50
55021.463	-53.08	0.31	-40.59	0.50
55032.425	-52.77	0.31	-41.16	0.50
55045.389	-52.61	0.31	-41.96	0.50
55052.287	-51.60	0.31	-41.63	0.50
55061.360	-51.35	0.31	-42.48	0.50
55066.468	-51.19	0.31	-42.59	0.50
55080.285	-50.89	0.31	-42.69	0.50
55083.447	-50.71	0.31	-42.61	0.50
55092.313	-49.87	0.31	-43.20	0.50
55093.263	-50.51	0.31	-42.75	0.50
55094.434	-50.26	0.31	-43.87	0.50
55096.357	-49.96	0.31	-43.80	0.50
55099.413	-49.60	0.31	-44.33	0.50
55104.390	-49.10	0.31	-44.73	0.50
55105.390	-49.06	0.31	-44.09	0.50
55106.390	-48.42	0.31	-45.48	0.50
55113.390	-48.31	0.31	-45.75	0.50
55118.365	-48.90	0.31	-45.09	0.50
55119.365	-48.50	0.31	-45.18	0.50
55120.365	-48.25	0.31	-45.56	0.50
55124.340	-48.17	0.31	-45.34	0.50
55126.340	-48.46	0.31	-45.73	0.50
55137.315	-47.84	0.31	-46.13	0.50
55139.440	-47.00	0.31	-46.51	0.50
55141.315	-47.21	0.31	-46.91	0.50
55145.290	-47.08	0.31	-46.75	0.50
55153.258	-47.00	0.31	-47.01	0.50
55158.265	-46.91	0.31	-46.63	0.50
55161.240	-46.84	0.31	-46.38	0.50
55241.131	-42.89	0.31	-51.20	0.50
55241.155	-42.63	0.31	-52.18	0.50
55242.131	-42.60	0.31	-51.61	0.50
55242.140	-42.73	0.31	-52.00	0.50

Note. Two-component RV measurements of 21 Ari (HD 13872) from the AST.

and by adding to the data set the 51 two-component RV measurements from the TSU AST spectra that span 358 days, enabling a full three-dimensional orbit to be evaluated, including the distance to the system and component masses. There is a small, but insignificant, fit improvement if the companion is assumed to be around star A instead of star B. The eccentricity of the subsystem orbit is not well constrained due to the small signal size and the majority of the highest precision astrometry being along only one axis on the sky. Thus, the eccentricity is fixed at zero in the present analysis. The 2-Keplerian orbit model

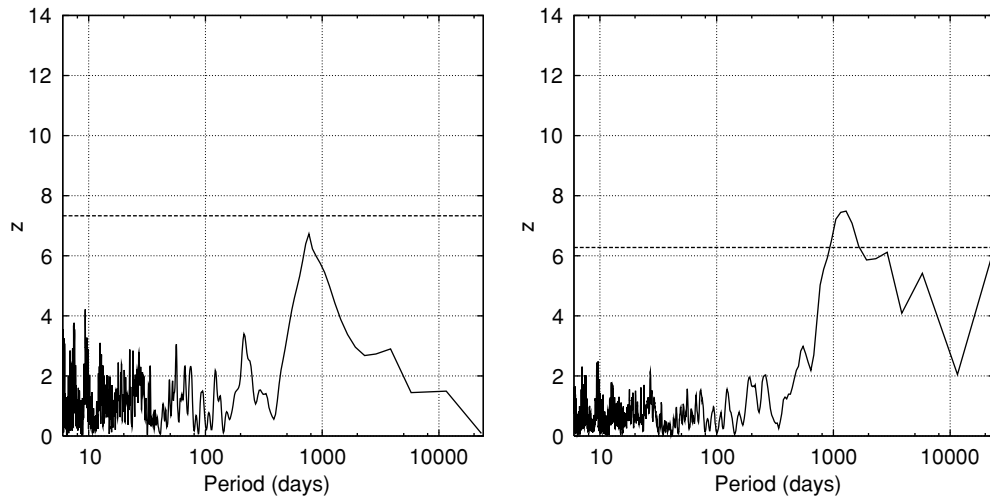


Figure 6. Periodograms of the F statistic comparing models with and without tertiary companions to HD 13872 (21 Ari) in astrometric-only models. The left figure is for analysis of only the PHASES data, while the right is for combined analysis of PHASES and non-PHASES astrometric measurements. For HD 13872 the 1% FAP is at $z = 7.33$ for the PHASES-only analysis, and $z = 6.27$ for the combined analysis, as indicated by horizontal lines.

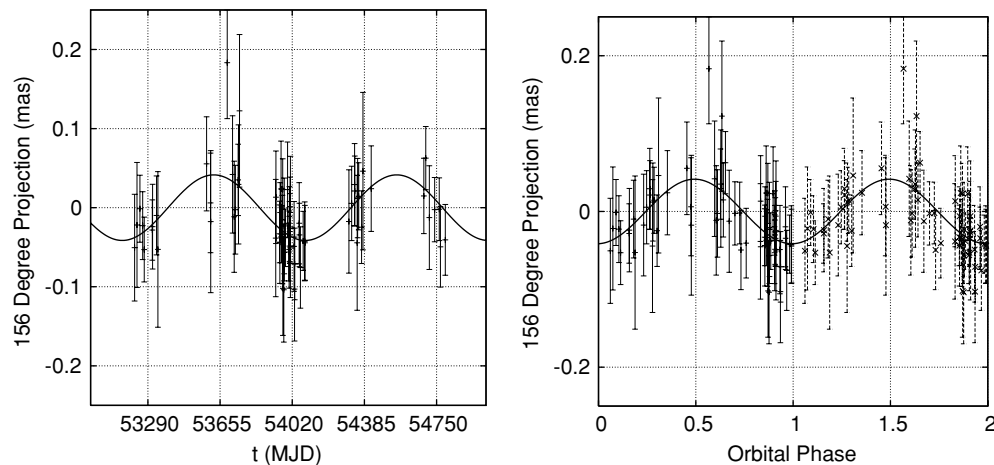


Figure 7. Motion of the center of light of the 925 day subsystem in HD 13872 (21 Ari) measured along an axis at angle 156° , measured from increasing differential right ascension through increasing differential declination; it was along this axis that the PHASES measurements were typically most sensitive for this binary. For clarity, only measurements with uncertainties along this axis of $100 \mu\text{as}$ or less are shown. Left: the center-of-light motion as a function of Modified Julian Date. Right: the center-of-light motion phase-wrapped about the orbital period and plotted covering two cycles.

is presented in Table 7. If real, the perturbation corresponds to a giant planet of mass $1.40 \pm 0.36 M_J$. The reflex motion of star A due to the presence of the companion is plotted in Figure 7 with the A–B binary orbit removed.

The model of HW99 predicts only planets with orbital periods less than 210 days will be stable. This is far smaller than the value of 925 ± 90 days that best fits the combined measurements. While the model from HW99 is broad in scope for generalized orbits, an analysis specific to the configuration of HD 13872 would be beneficial to explore whether there are additional islands of stability for companion orbital periods. However, the mutual inclination of the binary and planet orbits is not constrained well, limiting the utility of system-specific stability analysis. Clearly this cannot be considered a high confidence detection at this time.

Because the data are not of high enough quality to constrain the companion eccentricity, the FAP is greater than 0.1%, and the planet’s orbital period may be unstable according to the criteria of HW99, the reality of this planet is highly uncertain. HD 13872 will be an interesting object for continued study, but in this case it might not be surprising if future

observations do not confirm the presence of a giant planet in the system.

6.2. HD 202444

HD 202444 (τ Cyg, 65 Cyg, HR 8130, HIP 104887, WDS 21148+3803) is classified as an early F subgiant with a G dwarf companion. Various reports have suggested that the primary is a δ Scuti or γ Doradus variable, though these have not been confirmed.

The search for planetary companions to HD 202444 is more complicated than for other stars presented in this paper. It appears that a companion object may exist with an orbital period comparable to the span of PHASES observations (only two observations were taken outside of the 1155 day span from MJD 53234–54389 when most observations of reasonable cadence were made whereas the companion orbital period is over 800 days). Because the companion search software reoptimizes both the wide binary orbit model and the perturbing model every time a fit is made, the signal could be absorbed into that of the wider binary when only the shorter timespan PHASES data were

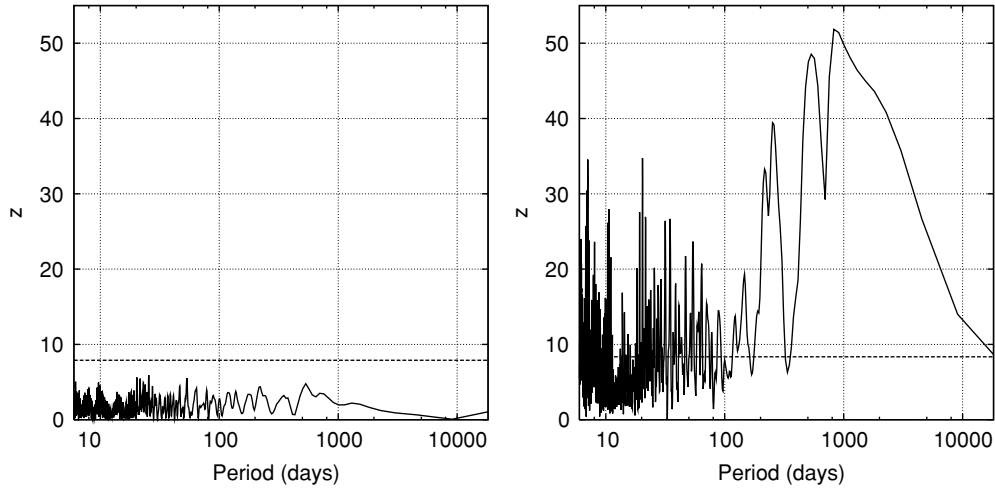


Figure 8. Periodograms of the F statistic comparing models with and without tertiary companions to HD 202444 (τ Ceti) in astrometric-only models. The left figure is for analysis only using the PHASES data, while the right is for combined analysis of PHASES and non-PHASES astrometric measurements. For HD 202444 the 1% FAP is at $z = 8.92$ for the PHASES-only analysis, and $z = 10.12$ for the combined analysis, as indicated by horizontal lines.

Table 7
Orbit Model for HD 13872

Parameter	Value	Uncertainty
P_{A-B} (days)	8622.7	4.4
T_{A-B} (MHJD)	46497.2	4.3
e_{A-B}	0.68119	0.00096
M_{Aa+Ab} (M_{\odot})	1.338	0.032
M_B (M_{\odot})	1.374	0.027
i_{A-B} (deg)	104.437	0.025
ω_{A-B} (deg)	263.927	0.031
Ω_{A-B} (deg)	55.823	0.032
P_{Aa-Ab} (days)	925	90
T_{Aa-Ab} (MHJD)	54092	62
e_{Aa-Ab}	0	(Fixed)
M_{Ab}/M_{Aa}	0.00100	0.00023
L_{Ab}/L_{Aa}	0	(Fixed)
i_{Aa-Ab} (deg)	71	45
ω_{Aa-Ab} (deg)	0	(Fixed)
$\Omega_{Aa-Ab,1}$ (deg)	211	55
$V_{0,AST}$ (kms^{-1})	-46.892	0.053
d (pc)	48.90	0.33
χ^2 and dof	406.1	471

Note. Best-fit orbital elements in the Campbell basis for HD 13872, with 1σ uncertainties.

analyzed. Thus, no compelling evidence for a companion was present when only PHASES measurements were analyzed—the initial PHASES-only search for companions found a most significant peak of $z = 5.93$ at a period of 25.5 days with FAP 19.1%. Analysis of the combined PHASES and non-PHASES data sets showed a larger value of χ^2 than one would have anticipated based on fits to the individual data sets, prompting a second search for tertiary companions, this time using all the astrometric measurements. When the non-PHASES measurements were added to the analysis, the extended coverage of the binary orbit prevented much of the ability to adjust the binary orbit to include the perturbations caused by possible companions. The revised search finds a very significant peak of $z = 51.85$ at a period of 826 days with FAP 0.0%. The orbit stability criteria of HW99 predict that companions with periods shorter than 2200 days are stable in HD 202444, which includes all candidate periods identified in the periodograms. The periodograms are plotted in Figure 8.

Table 8
Orbit Model for HD 202444

Parameter	Value	Uncertainty
P_{A-B} (days)	18125.4	7.7
T_{A-B} (MHJD)	47553	17
e_{A-B}	0.2392	0.0012
a_{A-B} (arcsec)	0.9130	0.0013
i_{A-B} (deg)	134.44	0.15
ω_{A-B} (deg)	298.77	0.19
Ω_{A-B} (deg)	339.75	0.13
P_{Ba-Bb} (days)	810	18
T_{Ba-Bb} (MHJD)	53139	48
e_{Ba-Bb}	0.43	0.17
a_{COL} (μas)	796	149
i_{Ba-Bb} (deg)	92.6	1.9
ω_{Ba-Bb} (deg)	90	19
$\Omega_{Ba-Bb,1}$ (deg)	78.7	2.5
χ^2 and dof	744.7	636

Note. Best-fit orbital elements in the Campbell basis for HD 202444, with 1σ uncertainties.

The orbit fitting was refined by seeding a full Keplerian fit with the best orbital parameters corresponding to the three largest peaks in the full data periodogram at periods 826, 534, and 252 days. The best fit occurred for the longest of these periods, for which the eccentricity of the subsystem orbit was constrained to be 0.43 ± 0.17 , so the full Keplerian model is accepted. The final fit has a subsystem period of 810 days, and the fit χ^2 is 744.7 with 636 degrees of freedom, compared to 994.7 and 643, respectively, for the single Keplerian fit. The best-fit two-Keplerian model parameters are presented in Table 8.

Since the companion is not detected when only the PHASES measurements or non-PHASES measurements are analyzed individually, there are reasons to doubt the authenticity of this proposed companion. Evidence for the companion only appears when the high-precision measurements are coupled with the measurements spanning more time. The reflex motion of the star in the subsystem is plotted in Figure 9, in which four measurements with uncertainties larger than $100 \mu\text{as}$ projected onto the selected axis are not shown; most of these points are consistent with this fit, though one suppressed measurement at MJD 53285 is a 5.4σ outlier. This measurement was taken

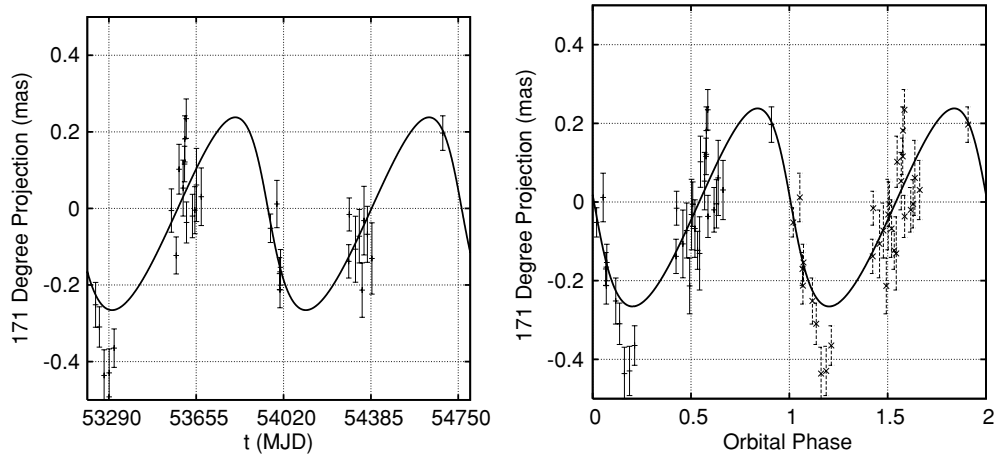


Figure 9. Motion of the center of light of the 810 day subsystem in HD 202444 (τ Cyg) measured along an axis at angle 171° , measured from increasing differential right ascension through increasing differential declination; it was along this axis that the PHASES measurements were typically most sensitive. For clarity, only measurements with uncertainties along this axis of $100\mu\text{as}$ or less are shown. Left: the center-of-light motion as a function of Modified Julian Date. Right: the center-of-light motion phase-wrapped about the orbital period and plotted covering two cycles for continuity.

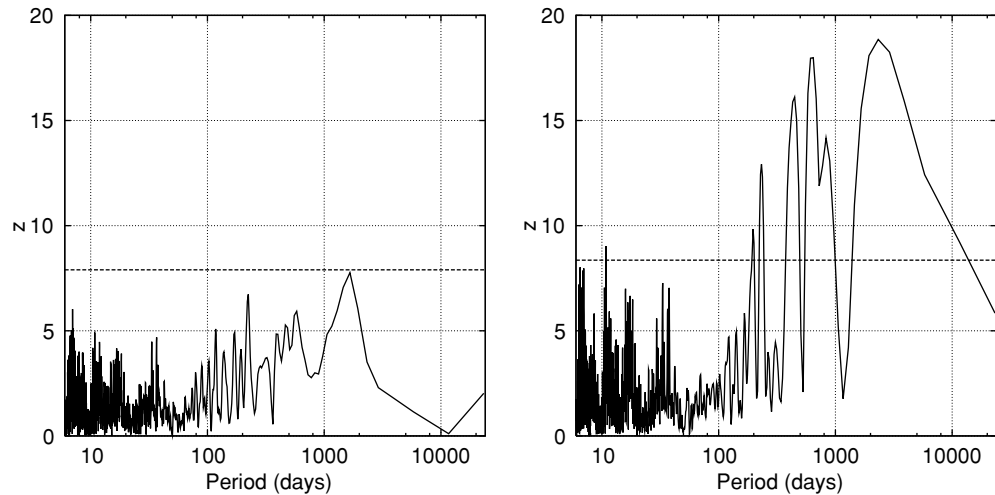


Figure 10. Periodograms of the F statistic comparing models with and without tertiary companions to HD 171779 (HR 6983) in astrometric-only models. The left figure is for analysis of only the PHASES data, while the right is for combined analysis of PHASES and non-PHASES astrometric measurements. For HD 171779 the 1% FAP is at $z = 7.90$ for the PHASES-only analysis, and $z = 8.36$ for the combined analysis, as indicated by horizontal lines.

with PTI's less reliable (and infrequently used) SW baseline, rather than the standard NS baseline. If the companion is a real object, it is at the border between the realm of brown dwarfs and giant planets, with a mass of $12.3 \pm 2.3 M_J$, for which a stellar mass of $1.36 M_\odot$ and a distance of 20.37 ± 0.25 pc have been assumed based on the work of S99. In case the candidate is not real, the single Keplerian binary-only orbit model was presented in Paper II. Continued high-precision observations of the system spanning at least five years would help clarify the situation.

7. SUBSTELLAR COMPANION CANDIDATES WITH AMBIGUOUS OR UNCERTAIN ORBITAL CHARACTERISTICS

7.1. HD 171779

HD 171779 (HR 6983, HIP 91013, WDS 18339 + 5221) was the first binary for which PHASES observations were published as a demonstration of the technique (Lane & Muterspaugh 2004). In total, 54 differential astrometric measurements were made at PTI of this pair of K giant stars.

The initial PHASES-only search for companions found a most significant peak of $z = 7.76$ at a period of 1663 days with FAP 1.4%. This low value inspired a revised search including both the PHASES and lower-precision non-PHASES astrometric observations to investigate whether the detection continued to be valid. The revised search finds a most significant peak of $z = 18.85$ at a period of 2328 days with FAP 0.0%. The periodograms resulting from these searches are presented in Figure 10. The two approaches find orbital periods within two samples of each other at $k = 5$ and $k = 7$, within the $f = 3$ oversampling factor of the search periods. Thus, the same signal is detected with both approaches. The stability criteria established by HW99 predict orbital periods up to 5200 days or more would be stable in this system. The best-fit Keplerian+circular subsystem orbital solution is presented in Table 9 and Figure 11.

However, this is not the only significant peak in the periodogram. In an attempt to uncover which of these might be a true signal, further efforts were made to refine the orbital fits with the subsystem orbital period seeded near 2328 days ($k = 5$), 647 days ($k = 18$), 448 days ($k = 26$), 831 days

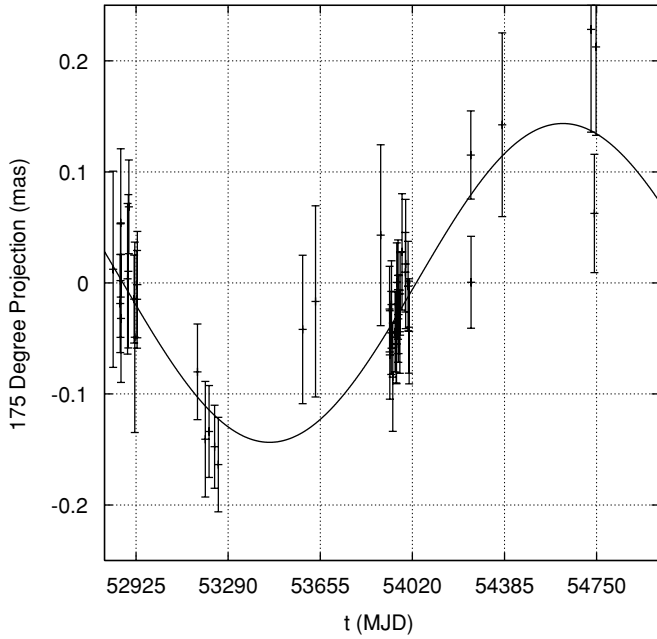


Figure 11. Time series of PHASES observations of HD 171779 (HR 6983) for the 2328 day subsystem orbital solution, measured along an axis at angle 175° from increasing differential right ascension through increasing differential declination; it was along this axis that the PHASES measurements are typically most sensitive. For clarity, only measurements with uncertainties along this axis of $100 \mu\text{as}$ or less are shown.

($k = 14$), and 233 days ($k = 50$). In all of these cases except for the 448 day selection, the eccentricity of the subsystem orbit could not be constrained by the astrometric measurements; in the case of the 448 day period, the best-fit non-zero eccentricity was 0.91 ± 0.34 , which is only poorly defined. Furthermore, visual inspection of the orbital fit to all but the 2328 day perturbation shows the others are almost certainly a result of observing cadence rather than a true periodic signal—see Figure 12. The 2328 day signal (refined to 2324 days after full orbit fitting) is slightly longer than the 1940 day span of PHASES observations, and the majority of the measurements might be best represented as a linear trend, though a circular orbital solution is also possible. If this corresponds to a real companion, the substellar object is either a very massive planet or a brown dwarf roughly 10 times the mass of Jupiter, assuming a distance of 196 pc (based on the revised *Hipparcos* parallax) and a stellar mass of $1.4 M_\odot$ (derived from the binary orbit).

The multiple peaks in the periodogram, potential for aliasing, inability to constrain the eccentricity of the companion, and best-fit orbit period being longer than the PHASES observation span prevent this detection from having high confidence. This system warrants further investigation over longer timespans to evaluate whether the detected perturbation is real and to constrain the orbit.

7.2. HD 196524

HD 196524 (β Del, 6 Del, HR 7882, HIP 101769, WDS 20375 + 1436) is a pair of F5 subgiants. The system is the brightest star in its constellation, despite being given the Bayer designation β . It and the fainter α Del were given proper names in the mid-1800s by Niccolò Cacciatore when he compiled the Palermo Star Catalogue; α and β Del have since been cataloged as Sualocin and Rotanev, respectively. These names are peculiar because they are the reverses of Nicolaus and Venator, the Latinized versions of Cacciatore’s own names (Allen 1963).

Table 9
Orbit Model for HD 171779

Parameter	Value	Uncertainty
P_{A-B} (days)	75200	2464
T_{A-B} (MHJD)	21156	295
e_{A-B}	0.4161	0.0083
a_{A-B} (arcsec)	0.2524	0.0072
i_{A-B} (deg)	48.0	1.4
ω_{A-B} (deg)	262.4	2.9
Ω_{A-B} (deg)	57.5	1.3
P_{Ba-Bb} (days)	2324	250
T_{Ba-Bb} (MHJD)	53375	21
e_{Ba-Bb}	0	(Fixed)
a_{COL} (μas)	160	48
i_{Ba-Bb} (deg)	66	21
ω_{Ba-Bb} (deg)	0	(Fixed)
$\Omega_{Ba-Bb,1}$ (deg)	157	33
χ^2 and dof	335.8	352

Note. Best-fit orbital elements in the Campbell basis for HD 171779, with 1σ uncertainties.

The initial PHASES-only search for companions found a most significant peak of $z = 7.76$ at a period of 6.81 days with FAP 1.9%. This value is somewhat suspicious since PHASES observations were often scheduled the same nights each week. However, a nearly equal height peak of $z = 7.53$ occurs at period 422 days, and yet another with $z = 7.46$ at 203 days. The presence of three peaks at very different orbital periods, potential for aliasing confusion in the peaks, and low FAP values inspired a revised search, including both the PHASES and lower-precision non-PHASES astrometric observations, to explore the sample of companion orbital periods to investigate whether the detection continued to be valid. The revised search finds a most significant peak of $z = 16.77$ at a period of 439 days with FAP 0.0%, within one sampling of the secondary peak in the original analysis. Furthermore, the peaks at ~ 200 and 6.81 days are still present, with values of $z = 15.88$ and $z = 12.88$, respectively. The periodograms are plotted in Figure 13.

Fits to double Keplerian models were seeded at the three potential companion orbital periods to explore which converged on the more satisfactory solution. The longest period model converged to a final orbital period of 435 days for a circular model with $\chi^2 = 1551.4$ and 1328 degrees of freedom. The full Keplerian version was unable to constrain the eccentricity and the fit failed. Analysis of the middle period solution was able to constrain modestly the eccentricity to $e = 0.67 \pm 0.24$ with a final $\chi^2 = 1549.1$ and 1326 degrees of freedom. Finally, the solution with a period near one week found a best-fit period of 6.8116 ± 0.0016 days for both circular and eccentric ($e = 0.27 \pm 0.28$) models, with $\chi^2 = 1570.5$ and $\chi^2 = 1570.2$, respectively.

Though 96 spectra of this system have been obtained by TSU’s AST, the spectral features of the two components were blended in all cases and could not be used for additional analysis. However, this does make it less likely that the 6.81 day signal is evidence of a real companion. The two longer period solutions are presented in Table 10 and Figures 14 and 15. The *Hipparcos*-based parallax of 32.5 ± 0.7 mas and average component mass of $1.67 M_\odot$ from S99 can be used to convert the stellar reflex motion to companion mass. If real, the 435 day companion would be a giant planet of 9 ± 1.6 times the mass of Jupiter whereas the 202 day companion would be a brown dwarf of 15 ± 3.9 times the mass of Jupiter.

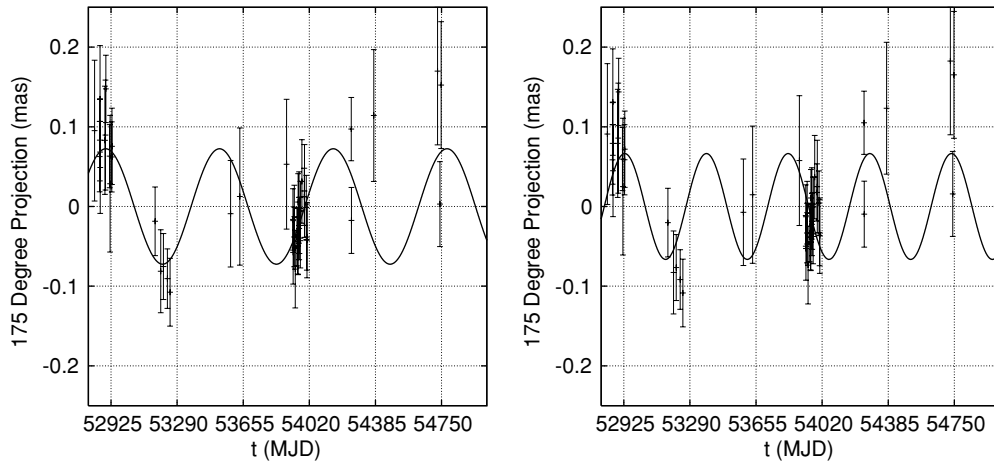


Figure 12. Time series of PHASES observations of HD 171779 (HR 6983) for two candidate orbital periods for companions to HD 171779, showing these solutions are likely due to cadence rather than an actual object. The best-fit model for the wide A–B binary motion based on a simultaneous fit with the perturbing model has been removed in each case, leaving only the motion of the center of light of the subsystem. Measurements are plotted along an axis at angle 175° , measured from increasing differential right ascension through increasing differential declination; it was along this axis that the PHASES measurements were most sensitive for this binary. For clarity, only measurements with uncertainties along this axis of $100 \mu\text{as}$ or less are shown. Left: the candidate orbital period is 628 days. Right: the candidate orbital period is 451 days.

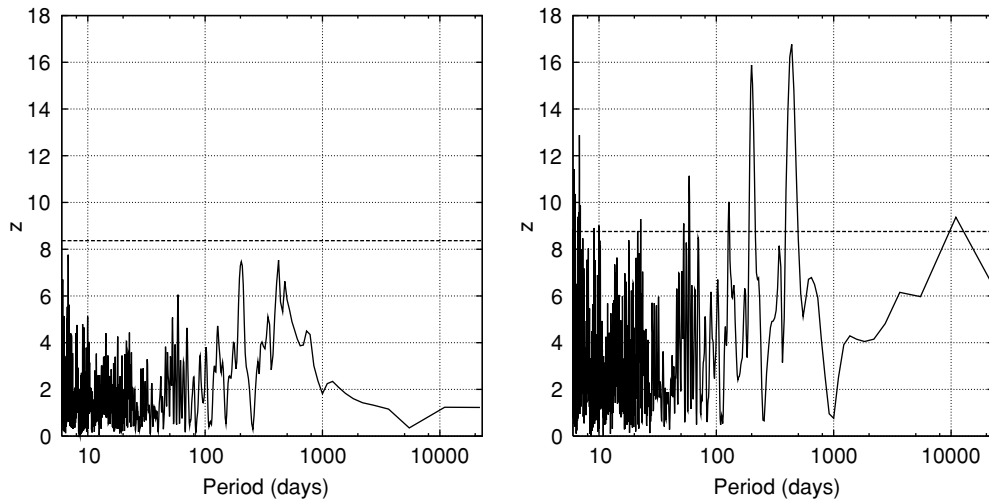


Figure 13. Periodograms of the F statistic comparing models with and without tertiary companions to HD 196524 (Rotanev/ β Del) in astrometric-only models. The left figure is for analysis of only the PHASES data, while the right is for combined analysis of PHASES and non-PHASES astrometric measurements. For HD 196524 the 1% FAP is at $z = 8.37$ for the PHASES-only analysis, and $z = 8.76$ for the combined analysis, as indicated by horizontal lines.

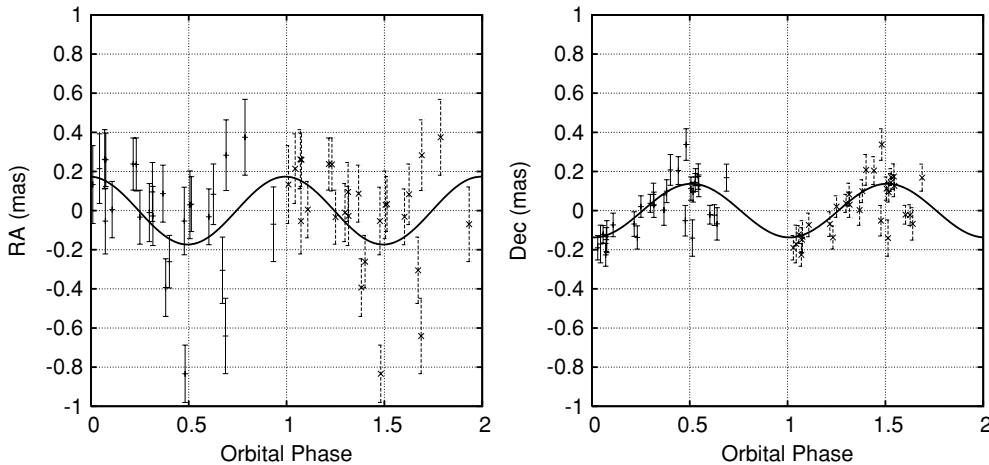


Figure 14. Phase-wrapped PHASES observations of HD 196524 (Rotanev/ β Del) for the longest candidate orbital period for a tertiary companion. The best-fit model for the wide A–B binary motion based on a simultaneous fit with the perturbing model has been removed, leaving only the motion of the center of light of the subsystem. Left: motion along the right ascension axis; for clarity, only measurements with uncertainties projected on the right ascension axis $200 \mu\text{as}$ or smaller are shown. Right: motion along the declination axis; for clarity, only measurements with uncertainties projected on the declination axis $100 \mu\text{as}$ or smaller are shown.

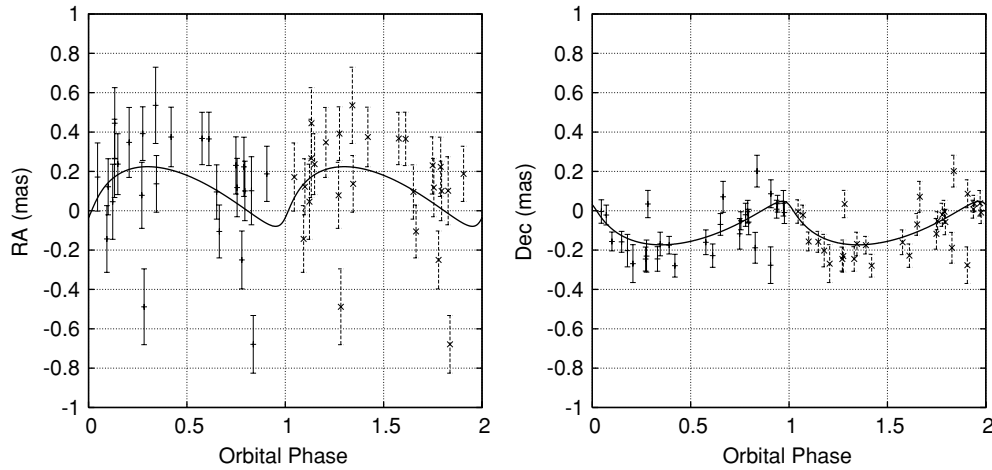


Figure 15. Phase-wrapped PHASES observations of HD 196524 (Rotanev/ β Del) for the 202 day candidate orbital period for a tertiary companion. The best-fit model for the wide A–B binary motion based on a simultaneous fit with the perturbing model has been removed, leaving only the motion of the center of light of the subsystem. Left: motion along the right ascension axis; for clarity, only measurements with uncertainties projected on the right ascension axis $200 \mu\text{as}$ or smaller are shown. Right: motion along the declination axis; for clarity, only measurements with uncertainties projected on the declination axis $100 \mu\text{as}$ or smaller are shown.

Table 10
Orbit Models for HD 196524

Parameter	Value	Uncertainty	Value	Uncertainty
P_{A-B} (days)	9745.6	1.4	9745.8	1.4
T_{A-B} (MHJD)	37960.0	4.1	37961.5	4.0
e_{A-B}	0.35632	0.00070	0.35595	0.00069
a_{A-B} (arcsec)	0.43676	0.00016	0.43701	0.00016
i_{A-B} (deg)	61.289	0.035	61.323	0.030
ω_{A-B} (deg)	168.81	0.14	168.86	0.13
Ω_{A-B} (deg)	357.206	0.033	357.179	0.029
P_{Ba-Bb} (days)	435.3	5.6	201.9	1.1
T_{Ba-Bb} (MHJD)	52941	20	53013.5	7.8
e_{Ba-Bb}	0	(fixed)	0.67	0.24
a_{COL} (μas)	221	40	217	57
i_{Ba-Bb} (deg)	87.2	4.6	84.3	3.4
ω_{Ba-Bb} (deg)	0	(fixed)	230	23
$\Omega_{Ba-Bb,1}$ (deg)	128.3	4.0	124.2	3.9
χ^2 and dof	1551.4	1328	1549.1	1326

Note. Possible orbits for HD 196524, in the Campbell basis with 1σ uncertainties.

At this point, it is not possible to distinguish whether either solution represents an actual companion, nor which model is preferred. Adding to the challenge of evaluating this system is the finding that for both solutions the perturbation orbit has an orientation on the sky that is more closely aligned with the major axis of the typical PHASES uncertainty ellipse. Where the signal is strongest, the astrometric precision is the worst. HD 196524 is a system that would benefit from continued observation by future astrometric efforts, especially those capable of truly two-dimensional measurements or that are sensitive to the perpendicular axis compared to PHASES.

8. CONTINUED STUDIES

Candidate substellar objects discovered by PHASES astrometry include

1. a planet slightly more massive than Jupiter around one of the stars in HD 176051,
2. one or more brown dwarfs around HD 221673,
3. a possible Jovian planet orbiting one of the stars in the HD 13872 system, though this has low confidence given

the non-zero FAP of the signal and the prediction that the orbit may not be stable over long periods of time,

4. a possible very massive planet or low-mass brown dwarf orbiting one of the stars in the HD 202444 binary, though this detection has reduced confidence because detection is not possible from PHASES measurements alone, but only reveals itself when lower precision astrometry covering longer time periods aid in constraining the binary orbit,
5. a possible very massive planet or brown dwarf companion in the HD 171779 system, though at present it is impossible to distinguish which of several possible orbital periods are correct, and
6. a possible massive planet or low-mass brown dwarf companion orbiting one of the stars in the HD 196524 system, though which of at least two possible orbital periods are correct cannot be determined at this time.

Of the 15 binary PHASES targets observed 10 or more times having semimajor axis in the 10–50 AU range, Paper III demonstrates the present data set cannot rule out planetary mass companions in any stable orbit for 4. Of the remaining 11 systems, there is strong evidence for a Jovian planet companion to HD 176051, while HD 13872 may also host a planet, though this detection is with lower confidence. Furthermore, the remaining nine systems in which no companions were detected but for which the constraints included some planetary mass companions (HD numbers 5286, 76943, 81858, 114378, 137107, 140436, 202444, 207652, and 214850) have a large range of unexplored orbital periods for which giant planetary companions cannot be ruled out. This implies that either the PHASES program was incredibly lucky, or giant planets are fairly common in close binary systems. The growing number of such systems being detected that are listed in Table 1 suggests that the latter explanation is more likely.

Thébaud et al. (2004) examined the formation of γ Cephei’s gas giant planet in the core-accretion scenario (Mizuno 1980), subject to the gravitational perturbations of the binary companion on a moderately eccentric ($e = 0.36$) orbit. Assuming a massive gaseous disk, they found that a $10 M_{\oplus}$ core could grow in ~ 10 Myr, but the core always formed at a distance of 1.5 AU, rather than at the observed 2.1 AU. Protoplanetary disks are seldom observed to survive for ~ 10 Myr around single young

stars, much less binary stars, making core accretion appear to be an unlikely formation mechanism for gas giants in relatively close binary star systems.

The alternative giant planet formation mechanism is disk instability (Boss 1997). Nelson (2000) modeled disk instabilities in an equal-mass binary system with semimajor axis $a = 50$ AU and eccentricity $e = 0.3$, but found that the disks became too hot to fragment into gas giant protoplanets. On the other hand, Mayer et al. (2005) found that disk instabilities could form gas giant planets in binary systems with $e = 0.14$ and $a = 116$ AU, but with $a = 58$ AU, whether fragmentation occurred or not depended on the protoplanetary disk masses and the assumed disk cooling rates. Boss (2006) found that disk instabilities could lead to giant protoplanet formation in binary systems with semimajor axes of 50 or 100 AU and eccentricities of 0.25 and 0.5. Mayer et al. (2007) tried to reconcile these disparate results for disk instability, but could only conclude that given the problems with core accretion and the observational fact that gas giants exist in binary star systems, disk instability remained as a possible formation mechanism for such planetary systems.

The candidate substellar companions discovered by PHASES require continued observations by other methods for confirmation. Because PTI ceased operations in 2008, acquiring new PHASES observations will not be possible. It is unlikely any existing northern hemisphere long baseline interferometers have the stable astrometric baselines required for differential astrometry, though the Navy Prototype Optical Interferometer may be a candidate site. However, it would be better if an independent method could be used. Recent work by Hełminiak et al. (2009) shows 40–1000 μas precision astrometry using adaptive optics (AO) on large telescopes, while Lazorenko et al. (2007, 2009) show similar precisions without AO on larger fields, which in principle might be applied to AO images capable of resolving the binaries. The PHASES candidate systems should be high priority targets for those observing programs; it is likely their precisions are sufficient to confirm or reject most of the candidate companions. The *SIM-Lite* Astrometric Observatory (Shao et al. 1995; Unwin et al. 2008) will also be capable of confirming these companions and identifying additional systems.

PHASES benefits from the efforts of the PTI collaboration members who have each contributed to the development of an extremely reliable observational instrument. Without this outstanding engineering effort to produce a solid foundation, advanced phase-referencing techniques would not have been possible. We thank PTI's night assistant Kevin Rykoski for his efforts to maintain PTI in excellent condition and operating PTI in phase-referencing mode every week. Thanks are also extended to Ken Johnston and the U. S. Naval Observatory for their continued support of the USNO Double Star Program. Part of the work described in this paper was performed at the Jet Propulsion Laboratory under contract with the National Aeronautics and Space Administration. Interferometer data were obtained at the Palomar Observatory with the NASA Palomar Testbed Interferometer, supported by NASA contracts to the Jet Propulsion Laboratory. This publication makes use of data products from the Two Micron All Sky Survey, which is a joint project of the University of Massachusetts and the Infrared Processing and Analysis Center/California Institute of Technology, funded by the National Aeronautics and Space Administration and the National Science Foundation. This research has made use of the Simbad database, operated at CDS, Strasbourg, France. M.W.M. acknowledges support from the Townes Fellowship Program,

Tennessee State University, and the state of Tennessee through its Centers of Excellence program. Some of the software used for analysis was developed as part of the *SIM* Double Blind Test with support from NASA contract NAS7-03001 (JPL 1336910). PHASES is funded in part by the California Institute of Technology Astronomy Department, and by the National Aeronautics and Space Administration under grant no. NNG05GJ58G issued through the Terrestrial Planet Finder Foundation Science Program. This work was supported in part by the National Science Foundation through grants AST 0300096, AST 0507590, and AST 0505366. M.K. is supported by the Foundation for Polish Science through a FOCUS grant and fellowship, by the Polish Ministry of Science and Higher Education through grant N203 3020 35.

Facilities: PO:PTI, TSU:AST

REFERENCES

- Abt, H. A., Levy, S. G., & Sanwal, N. B. 1980, *ApJS*, **43**, 549
- Allen, R. H. (ed.) 1963, *Star Names. Their Lore and Meaning* (New York: Dover)
- Baize, P. 1962, *J. Obs.*, **45**, 117
- Bean, J. L., Seifahrt, A., Hartman, H., Nilsson, H., Reiners, A., Dreizler, S., Henry, T. J., & Wiedemann, G. 2010, *ApJ*, **711**, L19
- Benedict, G. F., et al. 2002, *ApJ*, **581**, L115
- Boss, A. P. 1997, *Science*, **276**, 1836
- Boss, A. P. 2006, *ApJ*, **641**, 1148
- Campbell, B., Walker, G. A. H., & Yang, S. 1988, *ApJ*, **331**, 902
- Colavita, M. M., et al. 1999, *ApJ*, **510**, 505
- Correia, A. C. M., Udry, S., Mayor, M., Laskar, J., Naef, D., Pepe, F., Queloz, D., & Santos, N. C. 2005, *A&A*, **440**, 751
- Couteau, P. 1967, *J. Obs.*, **50**, 33
- Couteau, P., & Morel, P. J. 1982, *A&A*, **105**, 323
- Cumming, A., Butler, R. P., Marcy, G. W., Vogt, S. S., Wright, J. T., & Fischer, D. A. 2008, *PASP*, **120**, 531
- Cumming, A., Marcy, G. W., & Butler, R. P. 1999, *ApJ*, **526**, 890
- Eaton, J. A., & Williamson, M. H. 2007, *PASP*, **119**, 886
- Eggenberger, A., Udry, S., Mazeh, T., Segal, Y., & Mayor, M. 2007, *A&A*, **466**, 1179
- Gatewood, G., & Eichhorn, H. 1973, *AJ*, **78**, 769
- Han, I., Black, D. C., & Gatewood, G. 2001, *ApJ*, **548**, L57
- Hartkopf, W. I., Mason, B. D., & Worley, C. E. 2001, *AJ*, **122**, 3472
- Hatzes, A. P., Cochran, W. D., Endl, M., McArthur, B., Paulson, D. B., Walker, G. A. H., Campbell, B., & Yang, S. 2003, *ApJ*, **599**, 1383
- Hełminiak, K. G., Konacki, M., Kulkarni, S. R., & Eisner, J. 2009, *MNRAS*, **400**, 406
- Henry, G. W., Marcy, G. W., Butler, R. P., & Vogt, S. S. 2000, *ApJ*, **529**, L41
- Hershey, J. L. 1973, *AJ*, **78**, 421
- Holman, M. J., & Wiegert, P. A. 1999, *AJ*, **117**, 621
- Howard, A. W., et al. 2010, *ApJ*, **721**, 1467
- Konacki, M. 2005a, *Nature*, **436**, 230
- Konacki, M. 2005b, *ApJ*, **626**, 431
- Kürster, M., et al. 2003, *A&A*, **403**, 1077
- Lagrange, A.-M., Beust, H., Udry, S., Chauvin, G., & Mayor, M. 2006, *A&A*, **459**, 955
- Lane, B. F., & Muterspaugh, M. W. 2004, *ApJ*, **601**, 1129
- Lazorenko, P. F., Mayor, M., Dominik, M., Pepe, F., Segransan, D., & Udry, S. 2007, *A&A*, **471**, 1057
- Lazorenko, P. F., Mayor, M., Dominik, M., Pepe, F., Segransan, D., & Udry, S. 2009, *A&A*, **505**, 903
- Lloyd, J. P., Martinache, F., Ireland, M. J., Monnier, J. D., Pravdo, S. H., Shaklan, S. B., & Tuthill, P. G. 2006, *ApJ*, **650**, L131
- Makarov, V. V., Beichman, C. A., Catanzarite, J. H., Fischer, D. A., Lebreton, J., Malbet, F., & Shao, M. 2009, *ApJ*, **707**, L73
- Mason, B. D., Wycoff, G. L., Hartkopf, W. I., Douglass, G. G., & Worley, C. E. 2001, *AJ*, **122**, 3466
- Mason, B. D., Wycoff, G. L., Hartkopf, W. I., Douglass, G. G., & Worley, C. E. 2010, <http://www.usno.navy.mil/USNO/astrometry/optical-IR-prod/wds/WDS>
- Mayer, L., Boss, A., & Nelson, A. F. 2007, arXiv:0705.3182
- Mayer, L., Wadsley, J., Quinn, T., & Stadel, J. 2005, *MNRAS*, **363**, 641
- Mazeh, T., Tsodikovich, Y., Segal, Y., Zucker, S., Eggenberger, A., Udry, S., & Mayor, M. 2009, *MNRAS*, **399**, 906

- McArthur, B. E., Benedict, G. F., Barnes, R., Martioli, E., Korzennik, S., Nelan, E., & Butler, R. P. 2010, *ApJ*, **715**, 1203
- Mizuno, H. 1980, *Prog. Theor. Phys.*, **64**, 544
- Mugrauer, M., & Neuhauser, R. 2005, *MNRAS*, **361**, L15
- Muterspaugh, M. W., Lane, B. F., Kulkarni, S. R., Konacki, M., Burke, B. F., Colavita, M. M., & Shao, M. 2010c, *AJ*, **140**, 1631 (Paper III)
- Muterspaugh, M. W., et al. 2008, *AJ*, **135**, 766
- Muterspaugh, M. W., et al. 2010a, *AJ*, **140**, 1646 (Paper IV)
- Muterspaugh, M. W., et al. 2010b, *AJ*, **140**, 1623 (Paper II)
- Muterspaugh, M. W., et al. 2010d, *AJ*, **140**, 1579 (Paper I)
- Nelson, A. F. 2000, *ApJ*, **537**, L65
- Perryman, M. A. C., et al. 1997, *A&A*, **323**, L49
- Pfahl, E., & Muterspaugh, M. 2006, *ApJ*, **652**, 1694
- Pichardo, B., Sparke, L. S., & Aguilar, L. A. 2005, *MNRAS*, **359**, 521
- Pourbaix, D. 2001, *A&A*, **369**, L22
- Pravdo, S. H., & Shaklan, S. B. 2009, *ApJ*, **700**, 623
- Pravdo, S. H., Shaklan, S. B., & Lloyd, J. 2005, *ApJ*, **630**, 528
- Queloz, D., et al. 2000, *A&A*, **354**, 99
- Shao, M., Livermore, T. R., Wolff, D. M., Yu, J. W., & Colavita, M. M. 1995, *BAAS*, **27**, 1384
- Söderhjelm, S. 1999, *A&A*, **341**, 121
- Thébaud, P., Marzari, F., Scholl, H., Turrini, D., & Barbieri, M. 2004, *A&A*, **427**, 1097
- Tokovinin, A. A. 1987, *Sov. Astron. Lett.*, **13**, 448
- Tokovinin, A. A., & Smekhov, M. G. 2002, *A&A*, **382**, 118
- Unwin, S. C., et al. 2008, *PASP*, **120**, 38
- van de Kamp, P. 1963, *AJ*, **68**, 515
- van de Kamp, P. 1969, *AJ*, **74**, 757
- van Leeuwen, F. (ed.) 2007, in *Astrophysics and Space Science Library*, Vol. 350, Hipparcos, the New Reduction of the Raw Data
- Zucker, S., Mazeh, T., Santos, N. C., Udry, S., & Mayor, M. 2004, *A&A*, **426**, 695